# Spectroscopy of the eclipsing binary BD-00 2862
## - possible multiplicity[1]

W. D i m i t r o v[1], N. Ż y w u c k a[2],
M. P o l i ń s k a[1], K. K a m i ń s k i[1], M. K. K a m i ń s k a[1]

[1] Astronomical Observatory Institute, Faculty of Physics, A. Mickiewicz University,
ul. Słoneczna 36, 60-286 Poznań, Poland
e-mail: dimitrov@amu.edu.pl
[2] Astronomical Observatory, Jagiellonian University, ul. Orla 171, 30-244 Kraków, Poland
e-mail: natti@oa.uj.edu.pl

### ABSTRACT

We present the first spectroscopic analysis of the eclipsing binary BD-002862. The All Sky Automated Survey light curves yield orbital period of the system of 2.15 d. The shape of the light curve reveals that the components are almost spherical and the binary is detached. The eclipses depths show significant difference of the components' temperature. We acquired spectra with 0.5-m telescope equipped with an echelle spectrograph. The spectra are dominated by the lines of the more luminous component, which is about five times more luminous than its close companion. Obtained radial velocities together with the light curves enabled us to obtain a model of the system using the Wilson-Devinney method. The mass ratio of the stars is 0.67 and the size of the semi-major axis is 8.6 $R_\odot$. The obtained masses of the eclipsing components are $M_1 = 1.08 \pm 0.03$ and $M_2 = 0.72 \pm 0.02$ $M_\odot$. The stars are not evolved and the radii are close to the main sequence values: $R_1 = 1.21 \pm 0.01$ and $R_2 = 0.71 \pm 0.01$ $R_\odot$. The evolutionary tracks show that the system is probably on the pre main sequence stage. The photometric pararallax yields distance of 131 pc, which is comparable with the one obtained by Gaia mission - 130 pc. We carried out a spectrum analysis for the main component, the obtained temperature is $5600 \pm 400$ K and the metallicity is [M/H]=$-0.30 \pm 0.20$. The star has a visual companion separated by about 12 arc seconds. The companion has proper motion comparable to the one of the main star. Additionally, its distance ($\sim 100$ pc) based on the photometric parallax is comparable with the distance of component A. Therefore, the companion is probably a part of the system. Its spectral type is M3 with the estimated mass of about 0.3 $M_\odot$.

**Key words:** *Stars: individual: BD-00 2862 - binaries: eclipsing*

## 1. Introduction

Most of the field stars (60-80 %) are binary or multiple. The multiplicity fraction is higher for those with higher mass (Duchêne 1999, Duquennoy et al. 1991,

---

[1]Based on PST1 spectroscopy and ASAS photometry

Fisher et al. 1992). Stars form in clusters inside collapsing molecular clouds. Both observations and simulations reveal that 100% of the zero age stars are part of binary or multiple systems. The statistics of multiplicity, hierarchy and parameters like masses, periods and sizes of the semi-major axes of the observed stars give constraints on the initial conditions in which stars form. Stellar formation is still a field of intense investigation. The latest observation results show two main processes responsible for the formation of multiple stars: core fragmentation – separations of $10^{3-4}$ au (Pineda & Offner et al. 2015) and disc fragmentation $10^{1.5-2.5}$ au (Tobin & Crater 2016). The most probable process responsible for the formation of the closest pairs, shrinking of the orbit to $10^{-1}$ au, are the Kozai – Lidov cycles with tidal friction. The latest results are presented in review papers by Tholine (2002), Zinnecker (2002), Bate (2004) and Moe & Di Stefano (2017). Since 2009 we started observations of multiples with eclipsing component. Spectroscopy enabled us to detect new components in those systems (Dimitrov et al. 2014, 2015 and 2017). The existence of the close eclipsing sub systems in the multiples allows us to determine the absolute parameters of the pairs.

The eclipsing binary BD-00 2862 was observed by All Sky Automated Survey (ASAS, Pojmański 1997). First data was acquired on January 1999. The light curves reveal that the object is a detached eclipsing binary system. The equatorial coordinates of the star are $\alpha = 14^h42^m44\overset{s}{.}4$ and $\delta = -00°39'55''$ (FK5) and the visual magnitude is $10\overset{m}{.}1$. Other designations of the system are: TYC 4985-74-1 and GSC 04985-00074. The visual-band depth of the main eclipse is $0\overset{m}{.}5$ and the secondary eclipse is shallow, with depth of about $0\overset{m}{.}1$. Two light curves are available in $I$ and $V$ band and the orbital period of the eclipsing binary is 2.1503 d (Pojmański & Maciejewski 2004). Agueros et al. (2009) gave the spectral type of the star GV 5 + K1 V. The corresponding temperatures are 5660 K and 5170 K, according to Pecaut & Mammajek (2013) tables. As stated in Ammons et al. (2006), the color temperature of the binary is 5404 K. The object is a known ROSAT source (Voges et al. 1999). The Tycho-Gaia Astrometric Solution (TGAS) catalogue yields measurement of the parallax for BD-00 2862. The obtained value is $7.71 \pm 0.29$ mas, which corresponds to the distance of $130 \pm 5$ pc (Gaia Collaboration et al. 2016; Lindgren et al. 2016). The metallicity of the star is $[\mathrm{Fe/H}] = -0.24$ and the color excess $E(B-V) = 0.006$ mag (Ammons et al. 2006). The star has a visual companion separated by $\sim 12$ arc sec and about 6.5 mag fainter. Figure 1 presents the close neighborhood of the star. The proper motions listed in Table 1 show that the visual companion could be dynamically connected to the eclipsing binary.
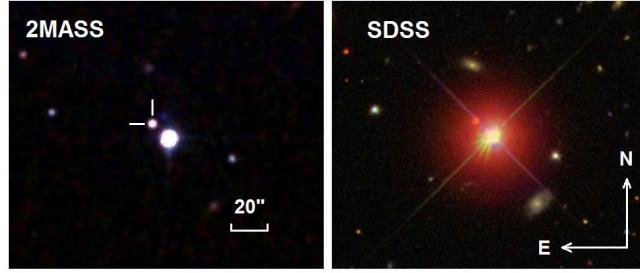
Fig. 1. The 2MASS and SDSS direct images of BD-00 2862. The visual companion B is marked on the left image.

T a b l e 1

Proper motions for BD-002862 (A) and the visual companion (B).

| source | comp. | $\mu_\alpha$ (mas/yr) | $\mu_\delta$ (mas/yr) | Ref. |
|--------|-------|----------|----------|------|
| GAIA DR1 | A | 5.98±1.42 | -65.79± 0.76 | Lindgren et al. 2016 |
| Tycho 2 | A | 8.2 | -64.8 | Hog et al. 2000 |
| FONAC | A | 8.6 | -68.8 | Kislyuk et al. 1999 |
| NPM1 | A | 8.6 | -64.9 | Klemola et al. 1987 |
| ASCC-2.5 V3 | A | 8.55 | -65.58 | Kharchenko et al. 2001 |
| URAT1 | A | 0.2 | -74.2 | Zacharias et al. 2015 |
| URAT1 | B | 2.9 | -72.3 | Zacharias et al. 2015 |
| UCAC4 | A | 6.9 | -66.1 | Nascimbeni et al. 2016 |
| UCAC5 | A | 6.7 | -64.5 | Zacharias et al. 2017 |
| UCAC5 | B | 13.7 | -52.2 | Zacharias et al. 2017 |
| mean value | A | 6.7±2.8 | -66.8±3.3 | |
| mean value | B | 8.3±7.6 | -62.3±14.2 | |

## 2. Data

### 2.1. Spectroscopy

Spectroscopic observations of the eclipsing binary BD-002862 were performed with Poznań Spectroscopic Telescope 1 (PST1) located in Borowiec at an elevation of 123 m above sea level, 52°16′37″ N, 17°04′29″ E (Baranowski et al., 2009). PST 1 consists of two Newtonian telescopes equipped with 0.5 m mirrors, with the focal length of 2.2 m. The first telescope is working in spectroscopic mode, while the second one in imaging mode. PST1 was designed to minimize light loses and to permit highly accurate RV measurements. The echellé spectrograph is equipped with 2048 × 2048 pixels Andor DZ 436 CCD camera. The spectrograph box is

thermally stabilized. The short-term stability reaches $\sim 35$ $m\,s^{-1}$, while the long-term stability is between 100 and 150 $m\,s^{-1}$. The main targets of the telescope are pulsating stars (e.g. Jerzykiewicz et al. 2013) and eclipsing binaries (e.g. Ratajczak et al. 2010).

The BD-002862 observations consist of 21 echellé spectra collected between April 2009 and June 2011 with the exposure time of 1800 s and spectral range of 4500 – 9240 Å in 2009 and 4300 – 7500 Å in 2011. The spectroscopic data were calibrated in wavelength with the use of the thor-argon spectra exposed before and after each object's spectrum.

The reduction process of BD-002862 spectra was performed using the IRAF[2] echellé package (D. Tody, 1986). Cosmic rays were removed from the spectra using an algorithm implemented by Pych (2004). The radial velocity (RV) of each spectrum was measured with IRAF FXCOR task, the spectra were correlated with a template using the cross-correlation method. As the secondary component peak is weak we used a late type template to enhance the signature of the less luminous star. The main source of RV errors is low SNR, especially in the weak secondary component's case.

T a b l e 2

Available photometric and spectroscopic data for BD-002862.

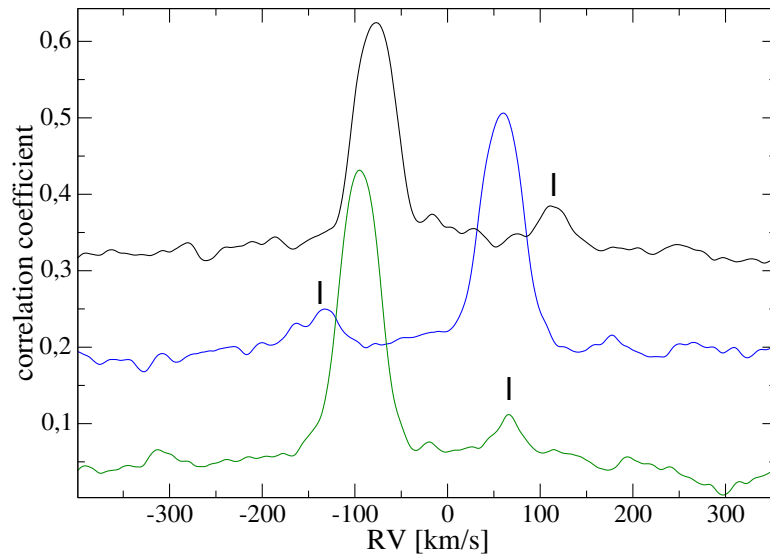| Instrument | HJD$_{start}$ $-2450000$ | HJD$_{end}$ $-2450000$ | Time span days | $n_{obs}$ |
|---|---|---|---|---|
| Photometry | | | | |
| ASAS *I* | 1200 | 1562 | 362 | 882 |
| ASAS *V* | 1919 | 4722 | 2803 | 378 |
| | | | | |
| Spectroscopy | | | | |
| PST1 (2009) | 4925 | 4937 | 12 | 12 |
| PST1 (2011) | 5643 | 5713 | 70 | 9 |

Fig. 2. Cross-correlation function of BD-00 2862 for different phases. The small peak of the secondary component is marked.
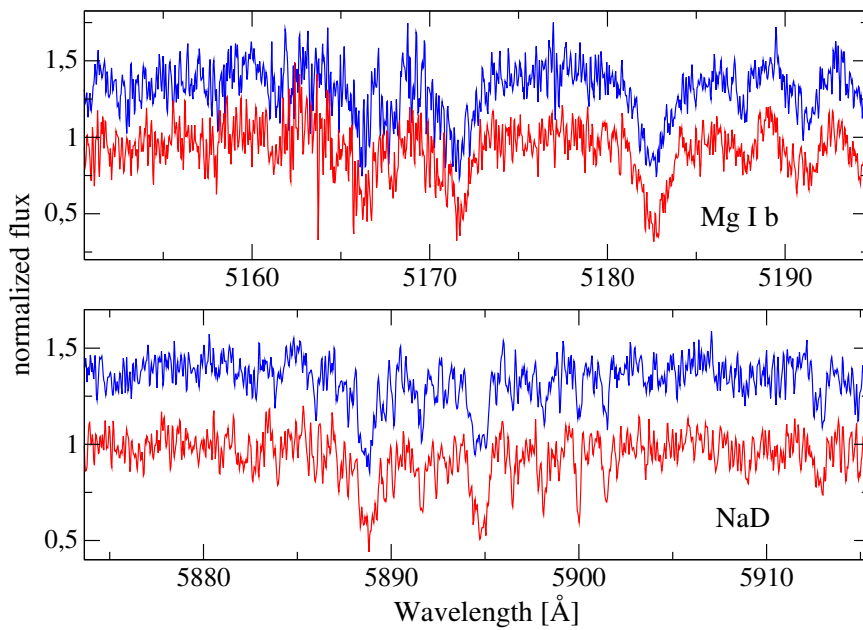


Fig. 3. Two spectral regions for two subsequent echellé spectra (red and blue) acquired on 30th May 2011. The orbital phase is close to the one with maximal radial velocity.

Radial velocity measurements obtained with the cross-correlation method.

| HJD −2450000 | RV$_1$ (km s$^{-1}$) | RV$_2$ (km s$^{-1}$) | RV$_3$ (km s$^{-1}$) |
|---|---|---|---|
| 4925.51447 | -63.0 | 95.4 | – |
| 4932.46391 | 46.6 | -59.5 | – |
| 4932.49133 | 50.6 | -70.0 | 16.4 |
| 4932.51881 | 59.2 | -77.4 | 13.8 |
| 4935.46610 | -9.7 | 19.6 | – |
| 4935.49224 | -12.7 | 15.3 | – |
| 4935.51883 | -10.5 | 26.3 | – |
| 4936.52779 | -2.0 | – | – |
| 4937.45197 | 42.4 | -51.6 | – |
| 4937.47871 | 36.8 | -43.7 | – |
| 4937.50477 | 31.2 | -34.9 | – |
| 4937.53143 | 26.0 | -25.1 | – |
| 5643.49620 | -78.4 | 121.7 | 21.3 |
| 5643.52095 | -78.1 | 121.9 | 21.5 |
| 5674.54003 | 81.4 | -115.3 | – |
| 5674.56404 | 82.5 | -115.3 | – |
| 5675.38665 | -44.9 | 72.7 | – |
| 5675.40287 | -47.7 | 78.7 | – |
| 5712.37483 | -72.8 | 118.2 | – |
| 5712.39853 | -70.6 | 116.1 | – |
| 5713.38389 | 80.6 | -123.6 | – |

## 2.2. *Photometry and Astrometry*

For modelling of the system (Sect. 3.3) we used photometry from The All Sky Automated Survey[3]. We used those data to calculate some moments of minima listed in Table 4. The ASAS survey is based on the wide-field 200/2.8 instruments for observations of stars brighter than 14 magnitude in $V$ and $I$ band. The eclipsing nature of BD-002862 was detected by ASAS. To determine is component B connected dynamically with A we used many catalogs containing astrometric data listed in Table 1.

**GAIA DR2** The latest GAIA results[4] for both components A and B are given in Table 4. Those values support hypothesis that B is part of BD-002862 system. The surrounding stars motion differs from the one of A and B components. The angular separation of the components is $11\overset{''}{.}36$.

---

[3]http://www.astrouw.edu.pl/asas/
[4]http://gaia.ari.uni-heidelberg.de/singlesource.html

T a b l e 4

The latest GAIA DR2 results for both A and B components.

| comp. | $\mu_\alpha$ (mas/yr) | $\mu_\delta$ (mas/yr) | parallax (mas) |
|-------|-----------------------|-----------------------|----------------|
| A | 7.54±0.08 | -65.69±0.07 | 7.99±0.05 |
| B | 8.70±0.17 | -66.39±0.14 | 7.90±0.10 |

## 3.  Results

### 3.1.  *The ephemeris*

Only one measurement of the main eclipse moment is available in the litera-ture (C. H. S. Lacy 2015). We have calculated more minima times based on the ASAS photometric and our RV data. The I band ASAS photometry was suitable for such measurements. We used PHOEBE SVN code for the measurements, fitting $HJD_0$ for small data sets. The results are listed in Table 4, the $O-C$ values were calculated with respect to the obtained ephemeris (Eq. 1). The $O-C$ values are comparable or lower than $1\sigma$ errors in determination of the $HJD_0$, which means that there is probably no light time effect in the system caused by a potential third body.

$$\mathrm{min\ \ I} = \mathrm{HJD}\ 2456715.9019(52) + 2.15027230(30) \cdot E \qquad (1)$$

### 3.2.  *Potential new components*

**The visual companion**   As mentioned in the introduction, the BD-00 2862 bi-nary has a visual companion B separated by about 12" (Fig. 1). According to the NOMAD catalog, the equatorial coordinates of the star are $\alpha = 14^h42^m45\overset{s}{.}0$ and $\delta = -00°39'47''$ (FK5) and the star's magnitude in the visual band is $16\overset{m}{.}68$. The position angle of the companion is about $45°$. In Table 1 we listed the re-sults of proper motion measurements from different sources. Those values are comparable for A and B components, which could therefore be dynamically con-nected. The projected distance between the components is about 1600 au. The NOMAD catalog lists the $H$ and $K$ band brightness of the companion. The color index is $H - K = 0.26$ mag and the corresponding visual absolute magnitude is $M_V = 11.63$, $T_{eff}$ about 3300 K and the spectral type is M3 V, assuming that the star is on the main sequence. This indicates that the companion is a very low mass star. The corresponding mass is about 0.3 M$_\odot$. We used Pecaut & Mamajek (2013) tables. The obtained photometric parallax of component B corresponds to a distance of about 100 pc, which is comparable to the GAIA distance of the A component (130 pc). This is subsequent argument in favor of the hypothesis that

Table 5

Times of minima.

| HJD$_0$ −2450000 | error days | cycles | O − C (d) | O − C (min) | instrument or source | $n_{obs}$ | Time span (d) |
|---|---|---|---|---|---|---|---|
| 1219.80451 | 0.00121 | 0 | -0.00142 | -2.0 | ASAS I | 20 | 4 |
| 1234.85761 | 0.00138 | 7 | -0.00023 | -0.3 | ASAS I | 37 | 6 |
| 1262.81026 | 0.00076 | 20 | -0.00112 | -1.6 | ASAS I | 55 | 6 |
| 1277.86255 | 0.00059 | 27 | -0.00073 | -1.1 | ASAS I | 74 | 6 |
| 1290.76742 | 0.00161 | 33 | 0.00250 | 3.6 | ASAS I | 23 | 3 |
| 1305.81881 | 0.00190 | 40 | 0.00199 | 2.9 | ASAS I | 61 | 6 |
| 1316.56806 | 0.00070 | 45 | -0.00013 | -0.2 | ASAS I | 59 | 6 |
| 1331.62093 | 0.00100 | 52 | 0.00084 | 1.2 | ASAS I | 71 | 6 |
| 4935.47839 | 0.00412 | 1728 | 0.00192 | 2.8 | PST1 (2009) | 9 | 12 |
| 5675.17364 | 0.00324 | 2072 | 0.00350 | 5.0 | PST1 (2011) | 9 | 70 |
| 6715.90120 | 0.00020 | 2556 | -0.00073 | -1.1 | Lacy (2015) | – | – |

component B could be dynamically connected with the main binary system A. The rough estimation of the orbital period of the A/B components, assuming that the orbit is perpendicular to the line of sight, yields $4.4 \cdot 10^4$ yr. In contrary to those results using other color indices, for example $J − K$ we obtained a significantly later spectral type. The object may have different color then a main sequence star because it could be very young (25-45, Section 4.1). The typical s/n in our spectra is 15-20. In case of the CCF anomalies s/n is 18 on 10th of April 2009 and 8 on 22nd March 2011.

**The third CCF peak**    Some spectra reveal an additional third peak in the correlation function. We found it in both data sets from 2009 and 2011. The peak is sharp and visible in subsequent spectra from two nights (See Fig. 3 and 4). The measured heliocentric velocities are listed in Table 1. We have verified whether the third peak could be connected with the telluric lines. We used spectral regions which avoid the Earth's atmospheric lines and the relative velocities are not close to 0; the measured values are $−12$ and $−16$ $km$ $s^{-1}$ for each date, respectively. Therefore, the peak is not connected with the telluric lines. It reveals small changes of the velocity between the two nights (Table 3). However, it is not present in most spectra, so it is hard to explain this peak with the presence of the third body in the system. The most probable explanation of this anomaly could be the chromospheric activity (Szczygiel 2008) or low S/N of the spectra. As we allready mentioned the object is a known ROSAT source.
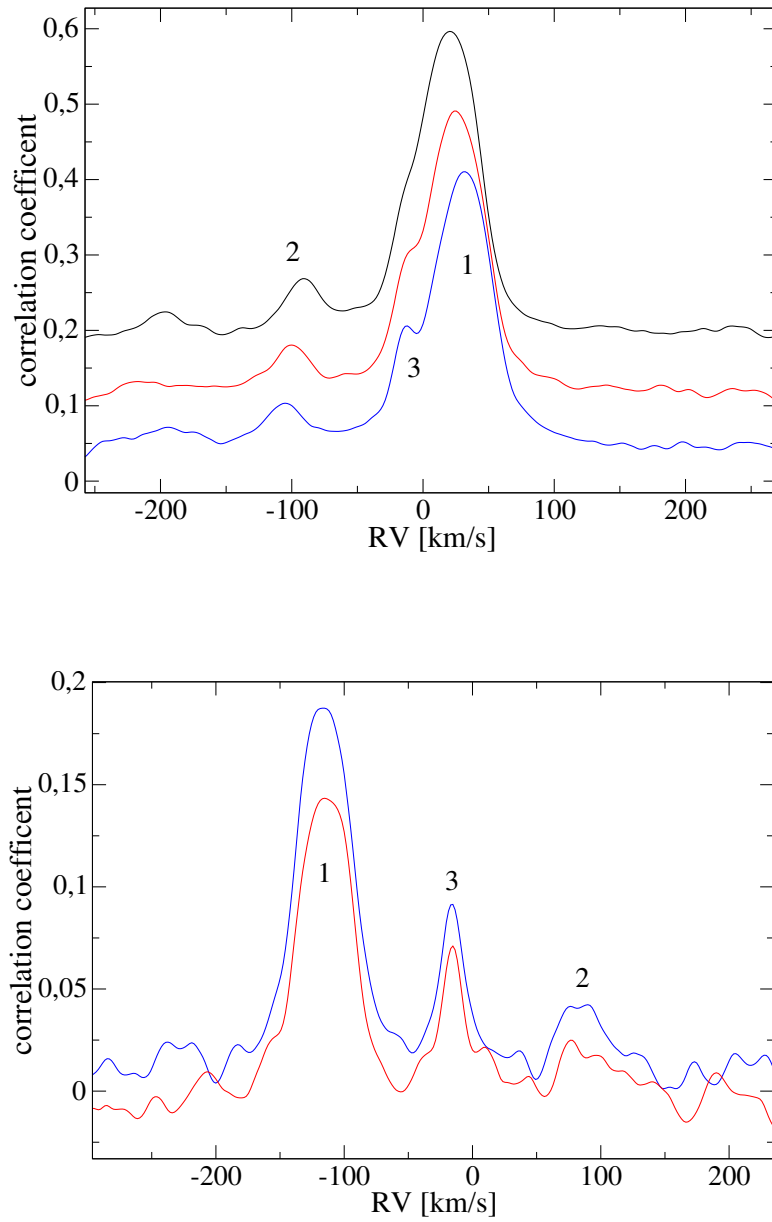
Fig. 4. The upper plot present three moving peaks of BD-00 2862 CCF on $10^{th}$ April 2009: 1, 2 - eclipsing pair, 3 -the third peak. The lower show cross-correlation functions for two subsequent spectra acquired on $22^{nd}$ March 2011.

### 3.3.   Model of the eclipsing pair

For modelling of the eclipsing pair we have employed the PHOEBE SVN code (Prša & Zwitter 2005) based on the Wilson-Devinney method (Wilson & Devinney 1971). We analyzed the ASAS *I* and *V* photometric data, as well as our radial velocity measurements. We assumed a circular orbit and synchronous rotation of both components. Both stars have convective envelopes, so we adopted albedoes of 0.5 and gravity brightening coefficients of 0.32. For calculation of the limb darkening effect we used the logarithmic law. Light curves reveal that the binary consists of two almost spherical stars - the LC maxima are flat. The primary and secondary eclipses have significant difference in depth, which is caused by different temperatures of the components.

The temperature of the main component was fixed on the value corresponding to the color of the system. We applied the Tycho unreddened color index. This is a good approximation, as the component one is about 5 times more luminous. This value is in good agreement with the spectral type of the binary G5 V + K1 V (Agueros et al. 2009). The temperature of the secondary component was fitted during the modelling. To ensure that we found a global minimum, we searched for alternative solutions. We used different starting points for fitting.

The final fit presents the two unevolved stars with masses of 1.1 and 0.7 M$_\odot$, the corresponding radii are 1.2 and 0.7 R$\odot$. The results are listed in Table 5. The stars are not distorted: the polar, point, side and back radii differ by less than 1% for both components. The final fit shows that the eclipses are total and have flat bottoms (Fig. 6). The projected rotational velocities, $v \sin i$, of both components are $28.3 \pm 0.1$ and $16.7 \pm 0.2$ km s$^{-1}$. We calculated the photometric parallax based on the temperatures and radii from Table 5. The obtained value is $7.64 \pm 0.26$ mas and the corresponding distance is $131 \pm 5$ pc, which is consistent with the Gaia result of $130 \pm 5$ pc. We take into account the extinction Av$= 0.002$ calculated from the color excess given by Ammons et al. (2006), but this value is negligible. The bolometric corrections were taken from Pecaut & Mamajek (2013).

### 3.4.   Evolutionary tracks

We calculated the evolutionary tracks for the two EB components. The Yonsei-Yale[5] results were used (Yi et al. 2001; Kim et al. 2002; Yi et al. 2003). The tracks are plotted in Fig. 9. The interpolation was made for metallicity $Z = 0.02$. We used the values of temperatures and surface gravity from the Wilson-Devinney model (Table 5). Both components lie close to the pre main sequence stage of the tracks. If the determination of the component temperatures is correct, the system is very young. The age of the components is about 25-45 Myr. Otherwise, if there are some systematic shifts in temperature determination of about 100-200 K, the components could be main sequence stars. The formation of multiples happens through cascade fragmentation. According to Machida et al. (2008) simulations,
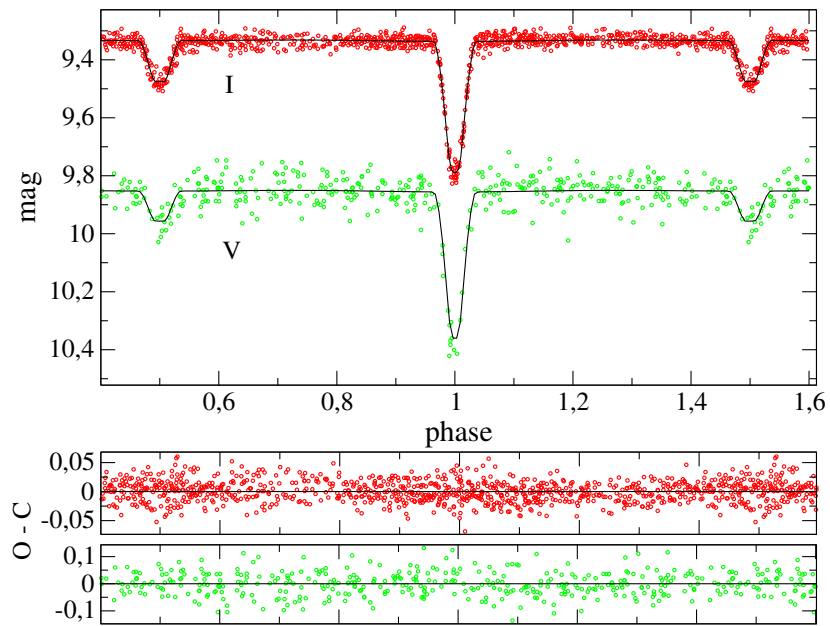
---

[5]http://www.astro.yale.edu/demarque/yystar.html

Fig. 5. ASAS photometric data compared with the fitted curves. The *V* band curve was shifted up by 0.3 mag. We only checked for I band data, because for the given band
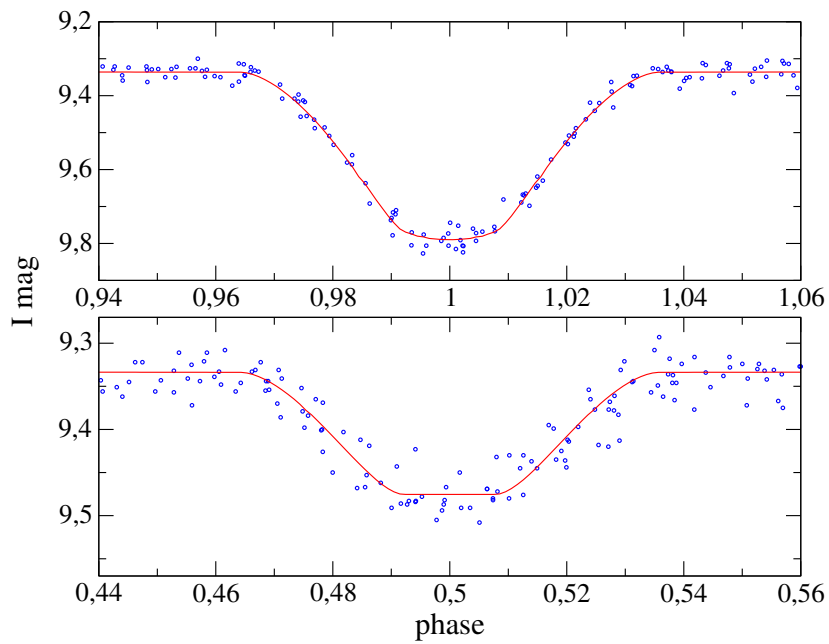


Fig. 6. The zoomed primary and secondary eclipse of the *I* band curve. The flat minima are clearly seen so we have total eclipses.

T a b l e 6

The derived model for the two components of the eclipsing pair.

| Parameter | component 1 | component 2 |
|-----------|-------------|-------------|
| *WD results* | | |
| $i$ | $88°39 \pm 0.08$ | |
| $q$ | $0.673 \pm 0.010$ | |
| $a$ $(R_\odot)$ | $8.552 \pm 0.061$ | |
| $V_\gamma$ (km s$^{-1}$) | $3.41 \pm 0.54$ | |
| | | |
| $\Omega_{1,2}$ | $7.78 \pm 0.04$ | $9.27 \pm 0.04$ |
| $l_{1,2}$ (I) | $0.881 \pm 0.002$ | $0.119 \pm 0.002$ |
| $l_{1,2}$ (V) | $0.913 \pm 0.005$ | $0.087 \pm 0.005$ |
| | | |
| *Absolute parameters* | | |
| $M_{1,2}$ $(M_\odot)$ | $1.085 \pm 0.030$ | $0.730 \pm 0.022$ |
| $R_{1,2}$ $(R_\odot)$ | $1.205 \pm 0.006$ | $0.710 \pm 0.007$ |
| $T_{eff\,1,2}$ (K) | $5633$ fixed | $4400 \pm 80$ |
| | | |
| $M_{bol\,1,2}$ | $4.44 \pm 0.07$ | $6.66 \pm 0.10$ |
| $\log g_{1,2}$ (cgs) | $4.31 \pm 0.016$ | $4.60 \pm 0.022$ |
| $v \sin i$ (km s$^{-1}$) | $28.3 \pm 0.1$ | $16.7 \pm 0.2$ |

the farther components like BD-00 2862 B separate in early isothermic phase of the cloud collapse. The rotation and turbulence enhance fragmentation, while the magnetic fields counteract this process. The eclipsing subsystem must form in late protostellar phase.

### 3.5.   *Atmospheric parameters of BD-002862*

Determination of atmospheric parameters requires high resolution spectra with good signal-to-noise ratio (S/N>100). In echelle spectra obtained with PST1 (R~35 000) the S/N is low, ranging from 10 to 25. These spectra also feature line profiles distorting near the merging points of consecutive echelle orders. All these factors influenced the uncertainty of the obtained parameters. The component BD-00 2862 is a eclipsing binary object whether its spectrum is dominated by the lines of the main component. As the S/N of our spectra is insufficient for spectrum analysis, we decided to investigate the averaged spectrum. The spectrum is dominated by the lines of the main component and we can treet it as a single lined spectrum in
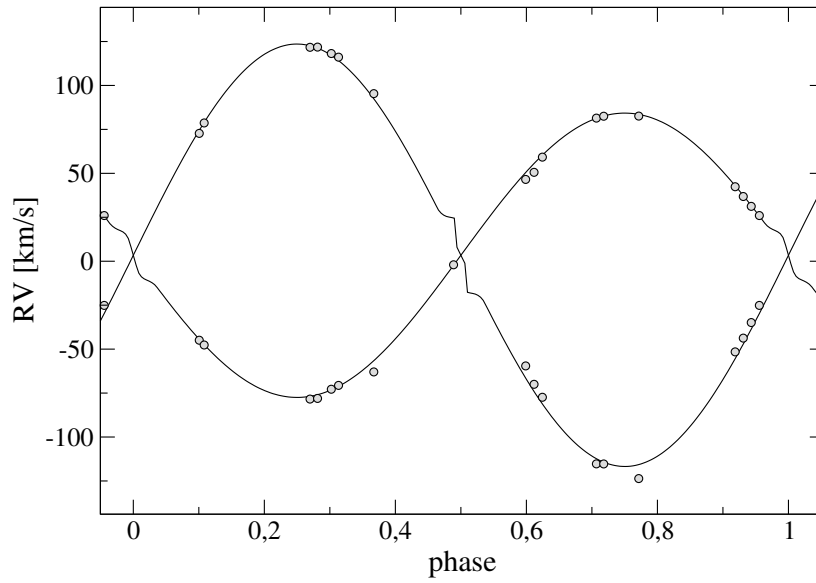
Fig. 7. Radial velocity curves of BD-00 2862. Circles present the measured velocities while the straight lines – synthetic RV curves.
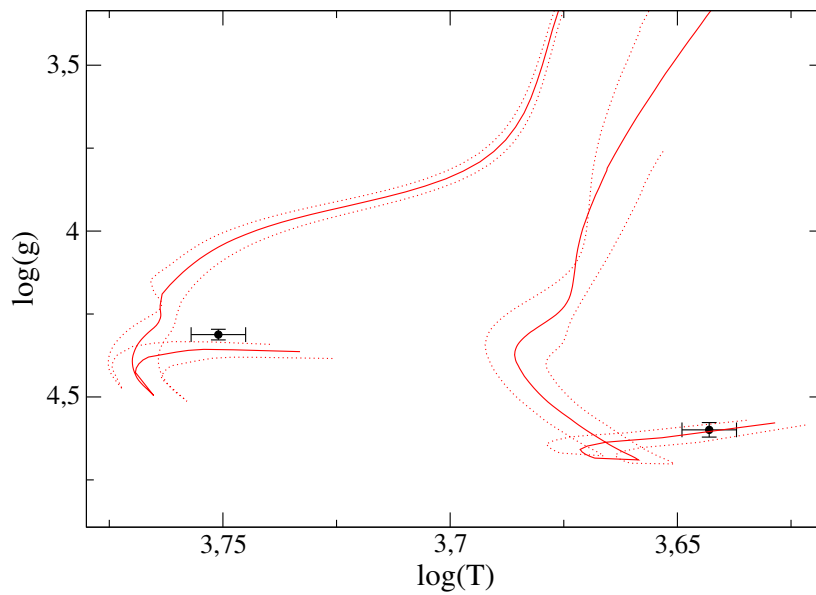


Fig. 8. The evolutionary tracks of the eclipsing pair components. Both stars are marked with black dots. The straight red lines present the tracks for 1.085 and 0.730 $M_\odot$ while the dotted lines show the error bars of mass determination.

our spectrum analisys.

To estimate atmospheric parameters (effective temperature, $T_{\rm eff}$, surface gravity, $\log g$, metallicity [M/H], and projected rotational velocity, $v \sin i$) the iSpec code (Blanco-Cuaresma et al., 2014) was used, adapting the same method as described in Dimitrov et al. (2017). The microturbulence and macroturbulence velocities were assumed as $1 \ {\rm km\, s^{-1}}$ and $0 \ {\rm km\, s^{-1}}$, respectively. The values of the microturbulence were chosen as typical for those types of stellar temperatures (Gray 2005). The macroturbulence velocities are related to $v \sin i$ and it is difficult to distinguish the two, especially from data with low S/N. Atmospheric parameters were calculated with synthetic spectral fitting technique using ATLAS9 grids of atmospheric models (Kurucz, 2005), the VALD database for atomic data (Kupka et al., 2011) and solar abundances were taken from Asplund et al. (2009).

For twelve selected spectra with S/N higher than 15 and different phases of orbital rotation, cross-correlation radial velocities were calculated and each spectrum was shifted relative to the synthetic spectrum with the iSpec code. The synthetic spectrum was generated for $T_{\rm eff}$, $\log g$ and $v \sin i$ values obtained from modeling of the system for component 1 (see Tab. 5), micro- and macroturbulence velocities were set to 1 and $0 \ {\rm km\, s^{-1}}$ and [M/H] = 0.0 dex. In the next step, the spectra were combined using the median flux values. The resulting signal-to-noise ratio for the received averaged spectrum was around 50. Comparison of the combined spectrum and a spectrum obtained on $2^{nd}$ April 2009 is shown in Fig. 10. Additionally, the continuum of spectra regions containing lines taken to determining atmospheric parameters was normalized.

To estimate the effective temperature, sensitivity of Balmer lines to this parameter was used. The received spectra cover the range 4500–9000 Å, hence only two Balmer lines, $H_\alpha$ and $H_\beta$, were used. During calculation parameter $\log g$ was set to 4.0 dex, while it does not affect Balmer line profile for stars cooler than $T_{\rm eff} \sim 8000$ K (Smalley, 2005). To evaluate uncertainties of $T_{\rm eff}$, we took into account the difference in temperatures calculated separately from the lines. The obtained value of the effective temperature was $5600 \pm 400$ K.

The next step was to estimate the surface gravity $\log g$ at the fixed $T_{\rm eff}$ value previously received. For calculations we have chosen the same, sensitive to gravity, spectral lines: Ca I (6162 Å), Na D (5890 Å and 5896 Å) and Mg I b (5167 Å, 5172 Å, 5183 Å), as described in Dimitrov et al. (2017). The best fit corresponds to $\log g$ = 3.8 ± 0.5 dex. The uncertainty of $\log g$ was derived from dispersion of the results calculated for individual lines. Metallicity [M/H] and projected rotational velocity $v \sin i$ were derived from spectral lines: Fe I (6431 Å), Fe II (6432 Å), and Ca I (6439 Å). The obtained values were [M/H] = -0.30 ± 0.20 dex and $v \sin i$ = 30 ± 4 $\rm km\, s^{-1}$. The comparison for the three regions of the average spectrum with synthetic spectra is presented in Fig. 12.
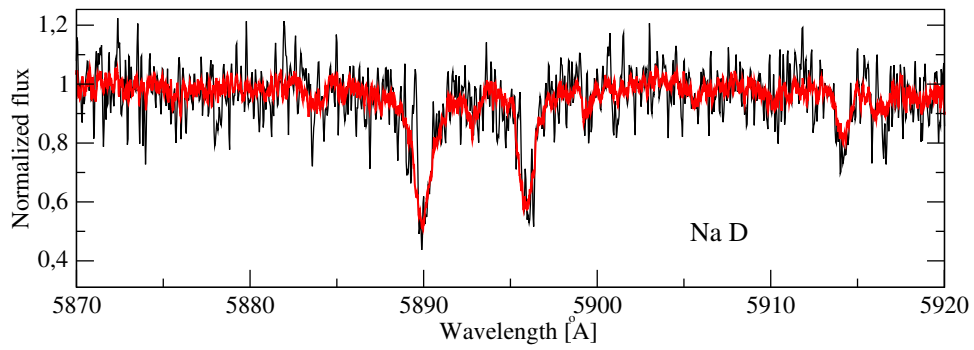
Figure 9: The combined average spectrum obtained from 12 spectra (red color) and for comparison one of the observed spectra (black color).
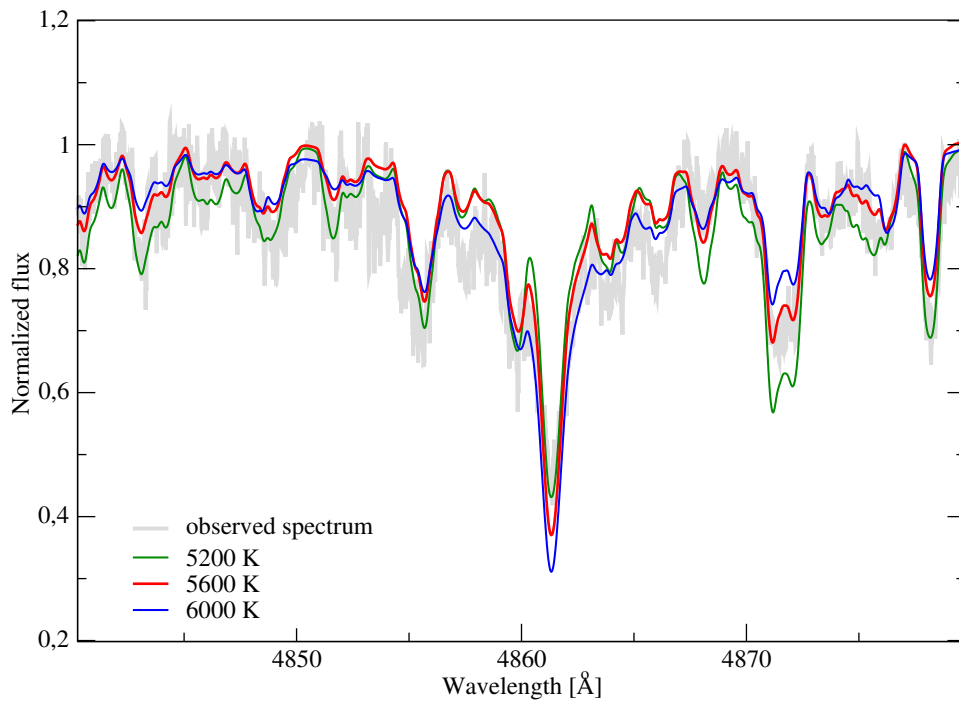


Figure 10: The comparison of the combined spectrum (gray color) and synthetic (with different colors) of the $H_\beta$ region. Different colors correspond to synthetic spectra calculated for various effective temperatures within the limits of error.

T a b l e 7

The atmospheric parameters obtained from spectrum synthesis
for the main component of BD-00 2862.

| $T_{\rm eff}[K]$ | $\log g$ [dex] | [M/H] [dex] | $v\sin i$ [km s$^{-1}$] |
|---|---|---|---|
| 5600±400 | 3.8±0.5 | -0.30±0.20 | 30±4 |
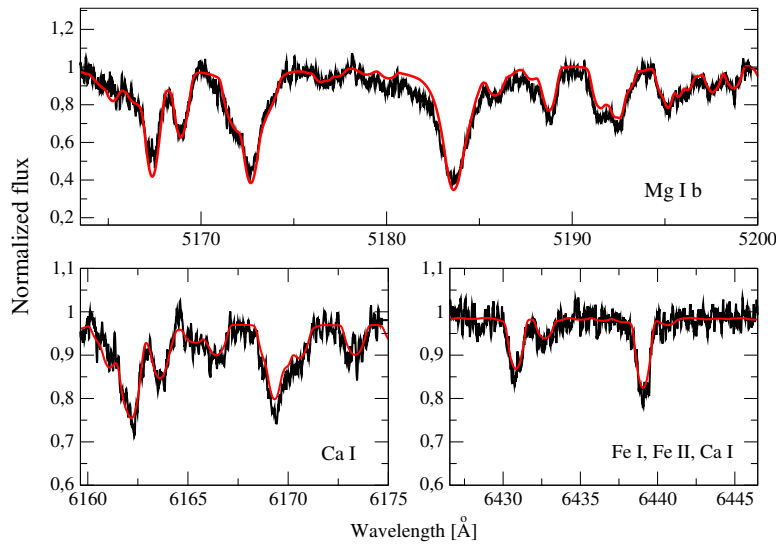


Figure 11: The combined spectrum (black) with the fitted spectrum (red) calculated
with the iSpec code for three line regions.

## 4. Conclusions

The analysis of BD-00 2862 system is based on our radial velocity observations,
ASAS photometry and other measurements from the catalogs. The results reveal
that the object is a triple star which consists of the main eclipsing binary and a far-
ther, visual third component. The star is not listed in the catalogs of visual binary
stars, we started to use designations A and B for both components. The measured
distance of component A, based on the trigonometric parallax method by Gaia and
photometric parallax based on our model are in very good agreement. The latest
GAIA DR2 results confirm that both A and B components have the same distance.
The arguments for the dynamical connection between component A and B, except
the small angular distance, are similar values of the proper motions and the dis-
tances. We used the photometric parallax method and infra-red color index H − K to

determine the distance of the visual companion. It is a low mass M3 spectral class star. Although, this result is uncertain because other color indices coresponds to significantly different values of the distance. We used a Wilson-Devinney method to calculate the model of the close eclipsing pair. The spectroscopic detection of the secondary component was on the limit of our telescope. Nevertheless, we were able to measure its velocities and to obtain radial velocity curves for both stars. We calculated the absolute parameters of the EB components with an accuracy of about 1 % for radii and 3 % for the masses.

# REFERENCES

Adelman-McCarthy, J., K., et al. 2009, *ApJS*, **182**, 543A.
Agueros, M., A., et al. 2009, *yCat*, **21810444A**, .
Ammons, S. M., Robinson, S. E., Strader, J., Laughlin, G., Fischer, D., and Wolf, A., 2006, *ApJ*, **638**, 1004.
Asplund, M., Grevesse, N., Sauval, A. J., and Scott, P. 2009, *ARA&A*, **47**, 481.
Baranowski, R., Smolec, R., Dimitrov, W., et al. 2009, *MNRAS*, **396**, 4.
Bate, M. R. 2004, *Rev. Mex. AA Ser. Conf.*, **21**, 175.
Blanco-Cuaresma, S., Soubiran, C., Heiter, U., and Jofré, P. 2014, *A&A*, **569**, A111.
Cutri, R., M. et al. 2003, *yCat*, **2246**, .
Duchêne G. 1999, *A&A*, **341**, 547.
Duquennoy, A., Mayor, M. 1991, *A&A*, **248**, 485.
Dimitrov, W., et al. 2014, *A&A*, **564**, A26.
Dimitrov, W., et al. 2015, *A&A*, **575**, A101.
Dimitrov, W., Lehmann, H., Kamiński, K., Kamińska, M. K., Zgórz, M., and Gibowski, M. 2017, *MNRAS*, **466**, 2.
Dimitrov, W., et al. 2018, *AcA*, **68**, 141.
Dommanget, J., and Nys, O., 1994, *Communications de l'Observatoire Royal de Belgique*, **115**, .
Fischer, D., A., Marcy., G., W. 1992, *ApJ*, **396**, 178.
Gaia Collaboration Brown, A. G. A., Vallenari, A., Prusti, T., de Bruijne, J. H. J., Mignard, F., et al. 2016, *A&A*, **special Gaia volume**, .
Gray, D. F., 2005, *The Observation and Analysis of Stellar Photospheres*, , .

Hog, E., et al. 2000, *A&A*, **355L**, 27H.

Jerzykiewicz, M., Lehmann, H., Niemczura, E., et al. 2009, *MNRAS*, **432**, 2.

Kim, Y.-C., Demarque, P., Yi, S. K., and Alexander, D. R., 2002, *ApJS*, **143**, 499.

Kharchenko, N.V., Roeser, S. 2001, *Kinematika Fiz. Nebesn. Tel.*, **17**, 409.

Kupka, F., and Dubernet, M.-L., VAMDC Collaboration 2011, *Baltic Astronomy*, **20**, 503.

Kurucz, R. L., 2005, *Memorie della Societa Astronomica Italiana Supplementi*, **8**, 14.

Klemola, A., R., Hanson, R., B., Jones, B., F. 1987, *AJ*, **94**, 501K.

Lacy, C., H., S., 2015, *Information Bulletin on Variable Stars*, **6130**, .

Lindegren, L., Lammers, U., Bastian, U., Hernández, J., Klioner, S., Hobbs, D., et al. 2016, *A&A*, **special Gaia volume**, .

Machida, M. N., Tomisaka, K., Matsumoto, T., and Inutsuka, S.-i., 2008, *ApJ*, **677**, 327.

Pecaut, M., J., & Mamajek, E., E., 2013, *ApJS*, **208**, 9.

Mason, B. D., Wycoff, G. L., Hartkopf, W. I., Douglass, G. G., and Worley, C. E., 2001, *AJ*, **122**, 3466.

Moe, M., & Di Stefano, R., 2017, *ApJS*, **230**, 15.

Pecaut, M., J., and Mammajek, E., E., 2013, *ApJS*, **208**, 9.

Pineda, Jaime E., Offner, Stella S. R., et al. 2015, *Nature*, **518**, 7538.

Pojmański, G., et al. 1997, *AcA*, **47**, 467.

Pojmański, G., & Maciejewski, G., 2004, *AcA*, **54**, 153.

Prša, A., and Zwitter, T., 2005, *ApJ*, **628**, 426.

Pych, W., 2004, *PASP*, **116**, 148.

Ratajczak, M., Kwiatkowski, T., Schwarzenberg-Czerny, A., et al. 2010, *MNRAS*, **402**, 4.

Smalley, B., 2005, *Memorie della Societa Astronomica Italiana Supplementi*, **8**, 130.

Szczygiel, et al. 2008, *AcA*, **58**, 405-418.

Tobin, John, J. and Kratter, Kaitlin, M., et al. 2016, *Nature*, **538**, 7626.

Tody, D., et al. 1986, *SPIE*, **627**, 733.

Tholine, J. E. 2002, *ARA&A*, **40**, 349.

Wilson, R. E., Devinney, E. J., 1971, *ApJ*, **166**, 605.

van Hamme, W., 1993, *AJ*, **106**, 2096.

Voges, W., et al. 1999, *A&A*, **349**, 389.

Yi, S., Demarque, P., Kim, Y.-C., Lee, Y.-W., Ree, C. H., Lejeune, T., and Barnes, S., 2001, *ApJS*, **136**, 417.

Yi, S. K., Kim, Y.-C., Demarque, P., 2003, *ApJS*, **144**, 259.

Zacharias, N., et al. 2015, *AJ*, **150**, 101Z.

Zacharias, N., Finch, C., Frouard, J. 2017, *AJ*, **153**, 166Z.

Zinnecker, H. 2002, *ASP Conf. Ser.*, **285**, 313.